Available online at www.sciencedirect.com
ScienceDirect
Trans. Nonferrous Met. Soc. China 25(2015) 879−884
Transactions of Nonferrous Metals Society of China
www.tnmsc.cn

Effects of Sn element on microstructure and properties of Zn−Cu−Bi−Sn high-temperature solder

Fei XING, Xiao-ming QIU, Yang-dong LI

Key Laboratory of Automobile Materials of Ministry of Education,
School of Materials Science and Engineering, Jilin University, Changchun 130025, China

Received 24 March 2014; accepted 14 July 2014

Abstract: The microstructures and properties of the Zn−Cu−Bi−Sn (ZCBS) high-temperature solders with various Sn contents were studied using differential scanning calorimetry (DSC), scanning electron microscopy (SEM) and X-ray diffraction (XRD). The results indicate that the increase of Sn content can both decrease the melting temperature and melting range of ZCBS solders and it can also effectively improve the wettability on Cu substrate. The shear strength of solder joints reaches a maximum value with the Sn addition of 5% (mass fraction), which is attributed to the formation of refined β-Sn and primary ε-$CuZn_5$ phases in η-Zn matrix. However, when the content of Sn exceeds 5%, the shear strength decreases due to the formation of coarse β-Sn phase, which is net-shaped presented at the grain boundary.

Key words: solder; Zn-based solder; Sn; high-temperature solder; thermal property; wettability

1 Introduction

The development of innovative materials has been putting new request to the soldering technology and solders, especially functional materials whose microstructures and properties are sensitive to the changing of temperatures, such as piezoelectric ceramic materials [1−3] and shape memory alloys [4−6]. When brazing these materials with filler metals, the severe joining temperatures (>500 °C) are always above the transition temperatures and will directly lead to the magnetic transformation and reduction of shape memory properties. In comparison with brazing, when soldering these functional materials below 350 °C, the joining temperature and mechanical properties are usually far from the basic needs in production. Furthermore, the multi-step joining of complicated parts, e.g., heavy truck Cu radiator, also needs various melting temperature solders to avoid the remelting of seams. So, the solders with melting temperature between 350−500 °C are urgently needed to join these materials.

Zn itself has a melting temperature of 419.5 °C, and has a strong reaction with copper and steel. By alloying elements, the melting temperatures of Zn-based alloys can be adjusted to a suitable melting temperature between 350−500 °C. Among the various elements, Sn and Al are traditional additions to form Zn−Sn [7,8] and Zn−Al [9,10] solders, which are widely used in the electric packaging and Al alloys soldering.

However, the studies of Zn−Cu solders to join copper and steel at 350−500 °C are scarce in the literature [11].

In recent studies, by adding small amount of Cu, Bi and Sn elements in Zn alloys, a series of novel Zn−2Cu−1.5Bi−Sn (ZCB−Sn) high-temperature solders have been developed [12]. However, there is still a lack of optimization of Sn content for the ZCB−Sn high-temperature solders. So the purpose of this work is to better understand the effects of Sn on the thermal properties, microstructure, wettability and mechanical properties of solder joints, and determine the optimal composition of ZCB−xSn (x=3%, 5%, 7%, mass fraction) high-temperature solders.

2 Experimental

Zn−2Cu−1.5Bi−xSn (ZCB−xSn) high-temperature solders were fabricated in nominal mass fraction compositions. Pure zinc, copper, tin and bismuth were

Foundation item: Project (20115003) supported by the Program for the Development of Science and Technology of Jilin Province, China
Corresponding author: Xiao-ming QIU; Tel: +86-15948385579; E-mail: qiuxm13@163.com
DOI: 10.1016/S1003-6326(15)63677-9

melted in a vacuum arc melting furnace to produce ZCB−*x*Sn (*x*=3%, 5%, 7%) high-temperature solders. The process of melting was carried out under high purity argon atmosphere with molten salt over the surface of the liquid solder to prevent oxidation. And then they were subsequently melted and cast into a quartz mold for cooling. The mass losses were measured to be less than 0.3% by high precision scale.

Differential scanning calorimetry (DSC) was used to determine the solidus and liquidus temperatures of the solders. The samples were examined under a nitrogen atmosphere. The kinetic curing profile was obtained by heating and cooling the formulated sample to the temperature of 500 °C at a rate of 10 °C/min.

The microstructure of ZCB−*x*Sn high-temperature solders was examined by optical microscopy (OM) and scanning electron microscopy (SEM). And the samples were etched in a solution with composition of $m(CrO_3):m(Na_2SO_4):m(H_2O)$=20:1.5:100 for 5 s. X-ray diffraction (XRD) was used to determine the phase component.

Wetting tests were carried out in accordance with the Chinese National Standard GB/T 11364—2008. The specimens of 0.3 g were cut, and put on the substrates covered with flux (20% $ZnCl_2$, 6% NH_4Cl, 3% NaCl and 2.5% LiCl solution), while the substrates were high conductivity Cu with size of 40 mm × 40 mm × 0.3 mm. The spreading areas were calculated using Auto CAD software, and the average data were used as the final results. In addition, a video-based contact angle meter (Data Physics Instruments GmbH, OCA20) was used to measure the contact angle of ZCB−Sn solders on Cu substrate. After soldering, the shear strength of joints was carried out in an electronic universal tester with a constant cross-head displacement rate of 0.5 mm/min, according to the Chinese National Standard GB/T 11363—2008. At least three samples were tested under each experimental condition.

3 Results and discussion

3.1 Thermal properties

Figure 1 shows the DSC heating curves of the high-temperature solder specimens with different contents of Sn elements. The solidus temperature (t_S), liquidus temperature (t_L) and melting range ($\Delta t=t_L-t_S$) of these alloys are calculated and presented in Table 1.

As given in Table 1, the liquidus temperatures are 400.1, 393.4 and 392.0 °C for ZCB−3Sn, ZCB−5Sn and ZCB−7Sn, respectively. With increasing the content of Sn from 3% to 7%, the liquidus temperature decreases 8.1 °C, and the declining tendency of solidus temperature is the same to liquidus temperature. Furthermore, it is found that the melting range decreases (from 9.6 °C to 6.8 °C) with the increase of the content of Sn from 3% to 5%, indicating that adding appropriate Sn content moves the near peritectic solder composition close to the peritectic value. Especially, the melting range of ZCB−5Sn high-temperature solder is very narrow, that is, less than 7 °C. This indicates that ZCB−5Sn solder has excellent thermal properties. Because the narrow melting range means that alloys exist as liquid for a short time during solidification and can avoid the tendency towards porosity and hot tearing, then form reliable joints in the reflowing process. For that reason, the ZCB−5Sn solder displays satisfactory reliability. Generally, the decrease in the melting point of ZCB−Sn solders could be possibly attributed to the increase of the surface instability and the variation in physical properties of the grain boundary/interfacial characteristics rendered by reinforcing intermetallic compound (IMC) phases. Hence, softening and dissolution of low-melting second phase particles are possible causes for the observed decrease in the melting point of the alloy solders, which brings down the melting temperature of ZCB−Sn high-temperature solders.

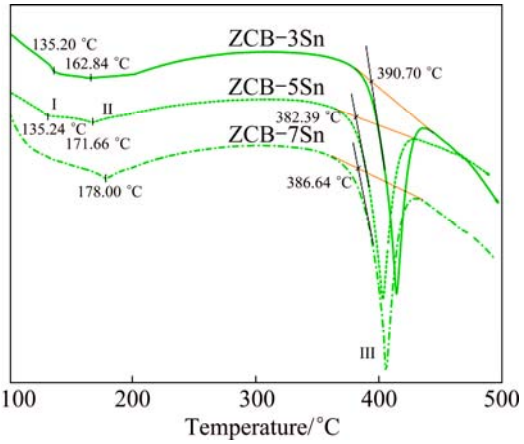

Fig. 1 DSC heating curves of ZCB−Sn solders

Table 1 Solidus, liquidus temperatures and melting range of ZCB−Sn solders

Alloy	*w*(Sn)/%	t_S/°C	t_L/°C	Δt/°C
ZCB−3Sn	3	390.7	400.1	9.4
ZCB−5Sn	5	386.6	393.4	6.8
ZCB−7Sn	7	382.4	392.0	9.6

From the DSC curves shown in Fig. 1, it is observed that the three curves are similar, with three main peaks at about 400, 170 and 135 °C, corresponding to the matrix peritectic reaction and pro-eutectic and eutectic transformations, respectively.

Based on the Zn−Cu and Sn−Bi phase diagrams and combined with the previous investigations [12], during the solidification of the experimental high-temperature solders, the primary ε-$CuZn_5$ phase firstly nucleates and

grows until the temperature falls to about 400 °C when peritectic reaction (L+ε-$CuZn_5$→η-Zn) occurs and then at 165−178 °C, the pro-eutectic β-Sn is formed from the reserved liquid phase (L→β-Sn). After that, a binary eutectic reaction (L→β-Sn+Bi) occurs at about 135 °C. In addition, it is found from Fig. 1 that no obvious eutectic peak at about 135 °C is observed in the heating curve of the solder with the addition of 7% Sn. This corresponds to the decrease of the amount of eutectic phase. With the increase of low-melting Sn addition, the solidification curve moves to the high-Sn content side, with large amount of β-Sn and little eutectic phases, according to the Sn−Bi binary phase diagram [13].

3.2 Microstructure

Figure 2 shows the representative micrographs of ZCB−Sn high-temperature solders. And the corresponding X-ray diffraction patterns of ZCB−Sn high-temperature solders are presented in Fig. 3. The microstructure of ZCB−Sn solder consists of light gray η-Zn matrix, black primary ε-$CuZn_5$, fiber-like β-Sn and white spherical Bi phases, as identified by EDS shown in Fig. 4.

With the addition of Sn increasing from 3% to 5% in the ZCB−Sn solder, it exhibits more uniform microstructure.

As shown in Fig. 2(b), the amount of β-Sn increases obviously, while that of coarse ε-$CuZn_5$ grains decreases. However, with the excessive addition of 7% Sn in the solder, fiber-like β-Sn phases become coarser and connect into nets (Fig. 2(c)).

With increasing the Sn content in ZCB−Sn high-temperature solders, the amount of pro-eutectic β-Sn increases while that of the ε-$CuZn_5$ decreases. Because the melting temperature of ε-$CuZn_5$ is much higher than that of β-Sn, the more the amount of β-Sn phases, the lower the melting temperatures of ZCB−Sn high-temperature solders, which is consistent with the results of the DSC analysis.

3.3 Wettability and mechanical property of joints

The developing in microstructure of the ZCB−Sn solders and the declining of melting temperature may result in changes to the wettability and mechanical properties of solder joints.

The wettability of ZCB−Sn high-temperature solders with various Sn contents was studied on Cu substrates. With the increase of Sn content from 3% to 7%, the spreading area of ZCB−Sn solders increases rapidly, from 186 mm^2 to 265 mm^2. A plot of the spreading area (S) versus Sn content is shown in Fig. 5. Linear regression analysis of the experimental data yields

$$S=112.900+20.004w(\text{Sn}) \quad (1)$$

Sn has an effect not only on the spreading area but also on the formability of ZCB−Sn high-temperature solders. Figure 6(a) shows the typical macrograph of ZCB−7Sn high-temperature solders on Cu substrate. It can be seen that the solder spreads greatly with a clear wetting ring in front and the contact angle is measured to be less than 5°.

As well known, the smaller surface tension components in the solution will gather together on the surface, which is so-called adsorption. And because of

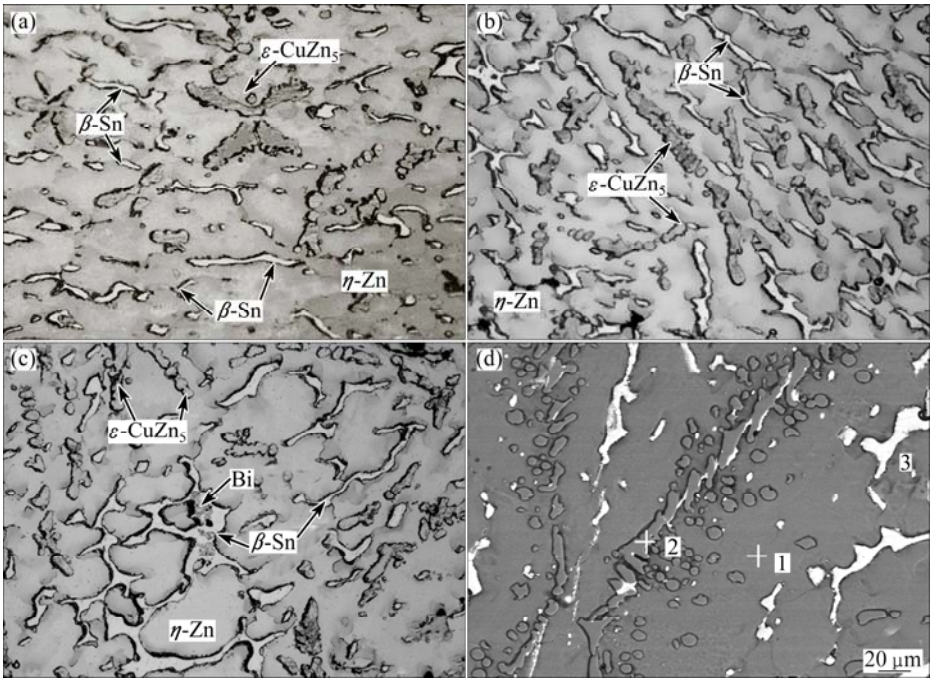

Fig. 2 Optical microstructures of ZCB−3Sn (a), ZCB−5Sn (b), ZCB−7Sn (c) solders and SEM microstructure (d) of ZCB−5Sn solder

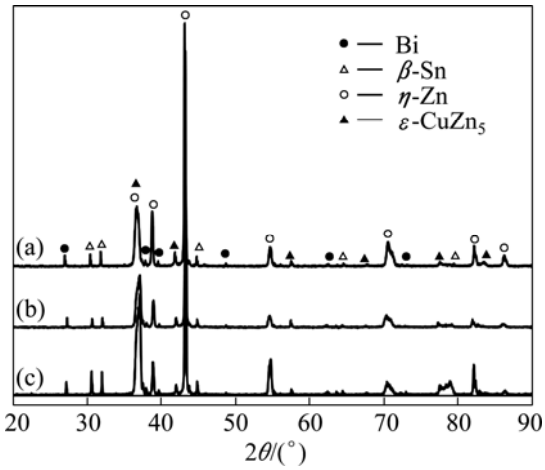

Fig. 3 XRD patterns of ZCB−3Sn (a), ZCB−5Sn (b) and ZCB−7Sn (c) solders

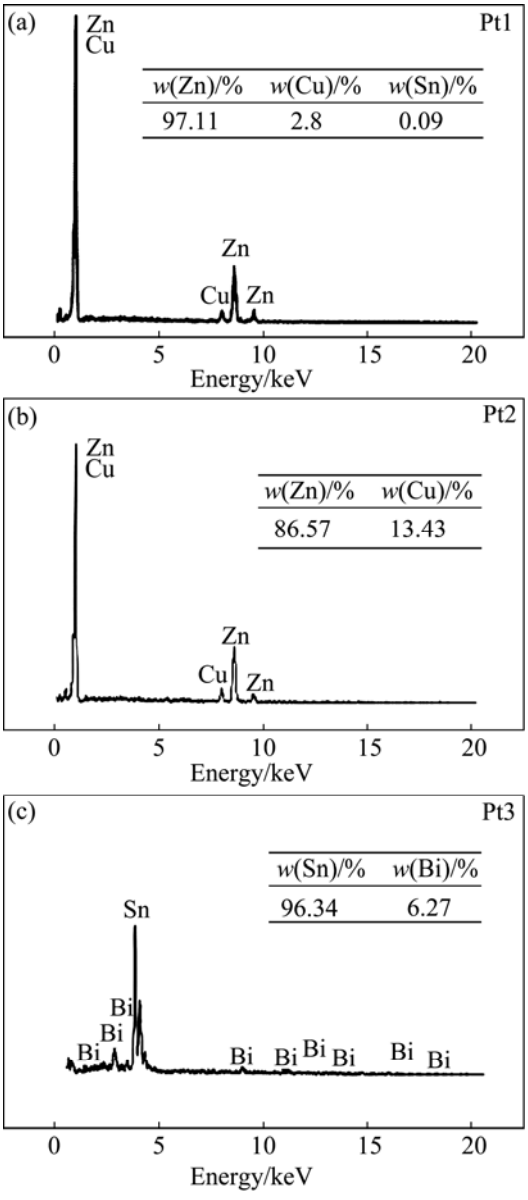

Fig. 4 EDS analysis results of ZCB−5Sn solder in Fig. 2(d)

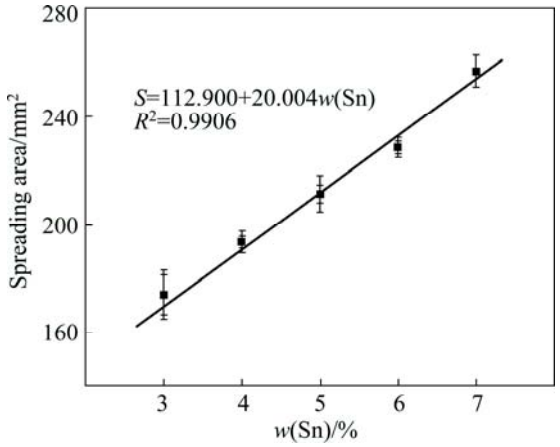

Fig. 5 Effect of Sn content on spreading area of ZCB−Sn high-temperature solders

the effect of adsorption phenomena, the surface and internal compositions of alloys are different, leading to the change of liquid surface tension (γ_0) [14]. As a given area, it is considered that the size of atoms between solute and solvent is different. So the larger the atom is, the more opportunity it occupies the surface. Because of the reasons mentioned above, γ_0 is used as parameter in dilute alloy solution, which means the smaller value of γ_0 leans to gather on the surface of liquid alloy [15]. That is

$$x_A^s/x_A = \exp[(\gamma_{0B} - \gamma_{0A})a/(RT)] \quad (2)$$

where x_A^s and x_A are the density of solute on the surface and internal of A, γ_0 is the surface tension, a is the average molar area of the surface atom. The surface tension of γ_{0Sn} is 0.7, which is much smaller than that of Zn (γ_{0Zn}=0.9) [15].

It means that Sn atoms are easier to gather on the surface. Moreover, with the increase of Sn content, the melting temperature of solders decreases, leading to the increase of flowability of solders at the same heating temperature [16]. As mentioned above, the increasing addition of Sn may decrease the surface tension of the solders, and finally improve the wettability. WU et al [17] reported that Bi atoms which are easier to gather on the surface could lead to the decrease of surface tension of Sn−9Zn alloys, and increase the wettability and strength of solder joints.

However, it should be on alert that the further increase of Sn in ZCB−Sn high-temperature solders may lead to the Sn segregation at the interface, and the joints would be easier to crack because of the stress concentration, as shown in Fig. 6.

Figure 7 shows the effect of Sn content on the shear strength of solder joints at a constant strain rate of 0.5 mm/min at room temperature. It can be seen that with the Sn content increasing from 3% to 5%, the joint shear strength increases dramatically from 32 MPa to 43 MPa.

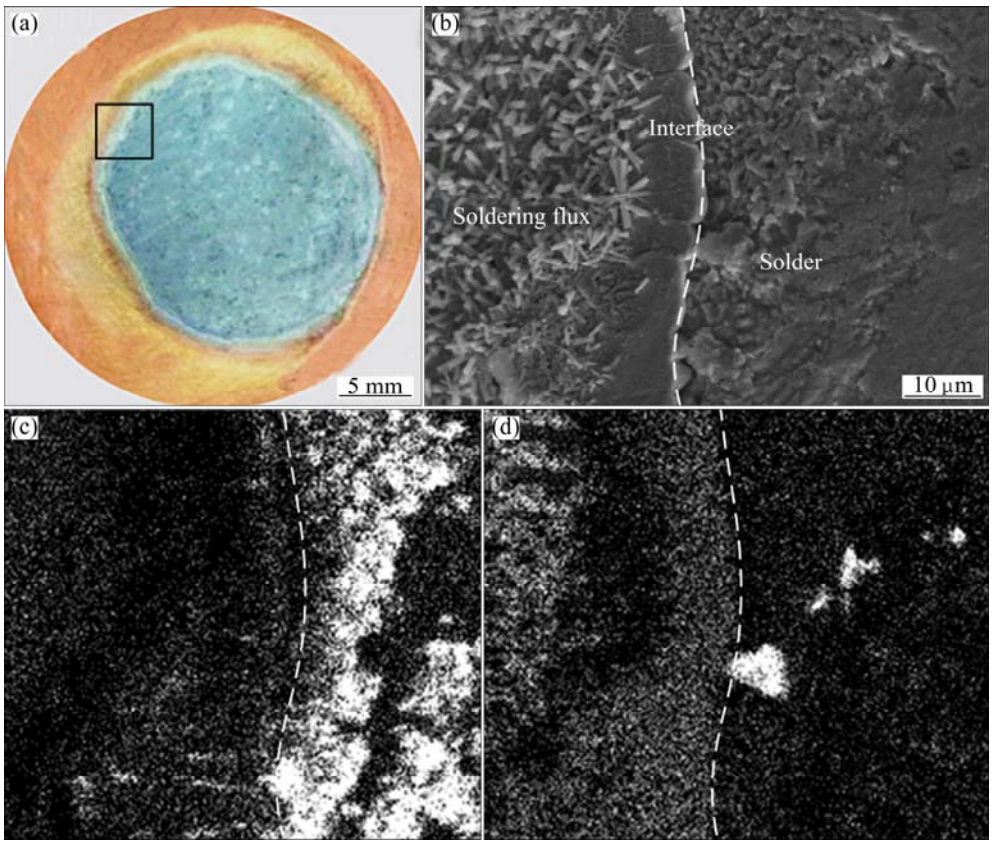

Fig. 6 Wetting morphology of ZCB−7Sn solder (a), SEM microstructure (b) and element Sn (c) and Cu (d) mappings of wetting interface

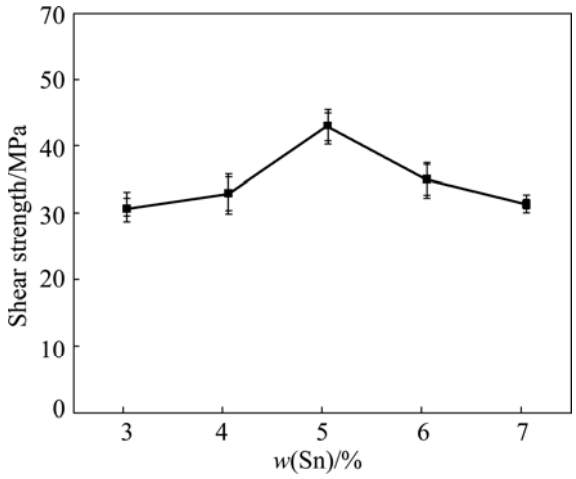

Fig. 7 Effect of Sn content on shear strength of solder joints

With further increase of Sn content, the shear strength of joint begins to gradually decrease.

According to the results of the thermal analysis, the microstructure observation and the properties of ZCB−Sn high-temperature solders, ZCB−5Sn high-temperature solder is suggested to joint copper at 350−500 °C, because of a much narrower melting range and more uniform microstructure, as well as higher shear strength of solder joints.

4 Conclusions

1) The addition of Sn decreases the melting temperatures and melting range temperatures of ZCB−Sn high-temperature from 400.1 to 392.0 °C and from 9.8 to 6.7 °C, respectively. Meanwhile, ZCB−5Sn high-temperature solder has the narrowest melting range temperature.

2) The appropriate addition of Sn favors the formation of refined primary ε-$CuZn_5$ and fiber-like β-Sn phases dispersed in η-Zn matrix.

3) With the increasing addition of Sn from 3% to 5%, significant improvement in the wettability and mechanical properties of the joints is realized. However, when the Sn content exceeds 5%, the shear strength of the joints decreases.

References

[1] RÖDEL J, JO W, SEIFERT K T P, ANTON E M, GRANZOW T. Perspective on the development of lead-free piezoceramics [J]. Journal of the American Ceramic Society, 2009, 92(6): 1153−1177.

[2] CHENG Hua-lei, ZHOU Wan-cheng, DU Hong-liang, LUO Fa, ZHU Dong-mei. Effects of dwell time during sintering on electrical properties of $0.98(K_{0.5}Na_{0.5})NbO_3$−$0.02LaFeO_3$ ceramics [J].

Transactions of Nonferrous Metals Society of China, 2013, 23(10): 2984−2988.

[3] DU Hong-liang, ZHOU Wan-cheng, LUO Fa, ZHU Dong-mei, QU Shao-bo, PEI Zhi-bin. Phase structure, dielectric properties, and relaxor behavior of $(K_{0.5}Na_{0.5})NbO_3$−$(Ba_{0.5}Sr_{0.5})TiO_3$ lead-free solid solution for high temperature applications [J]. Journal of Applied Physics, 2009, 105: 124104.

[4] KIM J, MIYAZAKI S. Effect of nano-scaled precipitates on shape memory behavior of Ti−50.9at.% Ni alloy [J]. Acta Materialia, 2005, 53(17): 4545−4554.

[5] ZHANG Yan-qiu, JIANG Shu-yong, ZHAO Ya-nan, TANG Ming. Influence of cooling rate on phase transformation and microstructure of Ti−50.9%Ni shape memory alloy [J]. Transactions of Nonferrous Metals Society of China, 2012, 22(2): 324−329.

[6] LI Ming-gao, SUN Da-qian, QIU Xiao-ming, SUN De-xin, YIN Shi-qiang. Effects of laser brazing parameters on microstructure and properties of TiNi shape memory alloy and stainless steel joint [J]. Materials Science and Engineering A, 2006, 424(1−2): 17−22.

[7] KIM S, KIM K S, KIM S S, SUGANUMA K. Interfacial reaction and die attach properties of Zn−Sn high-temperature solders [J]. Journal of Electronic Materials, 2009, 38(2): 266−272.

[8] MAHMUD R, ESLAM M. Shear strength of the Zn−Sn high-temperature lead-free solders [J]. Journal of Materials Science: Materials in Electronics, 2011, 22(8): 1168−1172.

[9] DAI Wei, XUE Song-bai, LOU Ji-yuan, LOU Yin-bin, WANG Shui-qing. Torch brazing 3003 aluminum alloy with Zn−Al filler metal [J]. Transactions of Nonferrous Metals Society of China, 2012, 22(1): 30−35.

[10] XIAO Y, JI H J, LI M Y, KIM J, KIM H. Microstructure and joint properties of ultrasonically brazed Al alloy joints using a Zn−Al hypereutectic filler metal [J]. Materials & Design, 2013, 47: 717−724.

[11] QIU Xiao-ming, YI Yun-chen, LIU Chun-shen. Investigation and application of XJ-1 Zinc-based filler metal [J]. Welding & Joining, 1993, 6: 5−7. (in Chinese)

[12] QIU Xiao-ming, XING Fei, MA Fei, BAI Yang. A novel middle-temperature ranged Zn-based solders to joining copper/steel and their preparation methods: CN 201110341677.8 [P]. 2013−10−16. (in Chinese)

[13] YU Jue-qi, Yi Wen-zhi, CHEN Bang-di, CHEN Hong-jian. Constitution of binary alloys [M]. Shanghai: Shanghai Science and Technology Press, 1987. (in Chinese)

[14] LIN Qing-zhi. Physical chemistry [M]. Beijing: Beijing Normal University Press, 2000. (in Chinese)

[15] SHI Lin. Thermodynamics of alloys [M]. Beijing: China Machine Press, 1992. (in Chinese)

[16] IIDA T, GUTHRIE R I L. The physical properties of liquid metals [M]. XIAN Ai-ping, WANG Lian-wen, transl. Beijing: Beijing Science and Technology Press, 2005. (in Chinese)

[17] WU Wen-yun, QIU Xiao-ming, YIN Shi-qiang. Influence of Bi, Ag on microstructure and properties of Sn−Zn lead-free solder [J]. The Chinese Journal of Nonferrous Metals，2006, 16(1): 158−163. (in Chinese)

元素 Sn 对 Zn−Cu−Bi−Sn 高温软钎料组织和性能的影响

邢 飞，邱小明，李阳东

吉林大学 材料科学与工程学院，汽车材料教育部重点实验室，长春 130025

摘 要：采用 DSC、SEM 和 XRD 等方法，研究 Sn 含量对新型 Zn−Cu−Bi−Sn 高温软钎料组织和性能的影响。结果表明：添加 Sn 可以明显降低钎料的固、液相线温度和熔化温度范围，并显著提高钎料的润湿性能。对钎料的显微组织分析发现，当 Sn 含量为 5%时，钎料的显微组织由均匀分布的细小 β-Sn 和初生 ε-$CuZn_5$ 相组成；此时，接头剪切强度达到最大。进一步增加钎料含 Sn 量，组织中出现大量粗化的网状 β-Sn 相，钎焊接头强度降低。

关键词：钎料；锌基钎料；Sn；高温软钎料；热学性能；润湿性

(Edited by Yun-bin HE)